Atmos. Chem. Phys. Discuss., doi:10.5194/acp-2016-1066, 2017
Manuscript under review for journal Atmos. Chem. Phys.
Published: 6 February 2017

A novel method to derive the aerosol hygroscopicity parameter based only on measurements from a humidified nephelometer system

Ye Kuang[1], ChunSheng Zhao[1], JiangChuan Tao[1], YuXuan Bian[2], Nan Ma[3], Gang Zhao[1]

[1]{Department of Atmospheric and Oceanic Sciences, School of Physics, Peking University, Beijing, China}

[2]{State Key Laboratory of Severe Weather, Chinese Academy of Meteorological Sciences}

[3]{Leibniz Institute for Tropospheric research, Leipzig, Germany}

*Correspondence to: C. S. Zhao (zcs@pku.edu.cn)

Abstract

Aerosol hygroscopicity is crucial for understanding roles of aerosol particles in atmospheric chemistry and aerosol climate effects. Light scattering enhancement factor $f(\mathrm{RH},\lambda)$ is one of the parameters describing aerosol hygroscopicity which is defined as $f(\mathrm{RH},\lambda) = \sigma_{sp}(RH,\lambda)/\sigma_{sp}(dry,\lambda)$ where $\sigma_{sp}(RH,\lambda)$ or $\sigma_{sp}(dry,\lambda)$ represents σ_{sp} at wavelength λ under certain RH or dry conditions. Traditionally, an overall hygroscopicity parameter κ can be retrieved from measured $f(\mathrm{RH},\lambda)$, hereinafter referred to as $\kappa_{f(\mathrm{RH})}$, by combining concurrently measured particle number size distribution (PNSD) and mass concentration of black carbon. In this paper, a new method is proposed to directly derive $\kappa_{f(\mathrm{RH})}$ based only on measurements from a three-wavelength humidified nephelometer system. The advantage of this newly proposed novel approach is that it allows researchers to estimate $\kappa_{f(\mathrm{RH})}$ without any additional information about PNSD and black carbon. Values of $\kappa_{f(\mathrm{RH})}$ estimated from this new method agree very well with those retrieved by using the traditional method, the average difference between $\kappa_{f(\mathrm{RH})}$ derived from newly proposed method and traditional method is 0.005 and the square of correlation coefficient between them is 0.99.

1. Introduction

Atmospheric aerosol particles play vital roles in visibility, energy balance and the hydrological cycle of the Earth-atmosphere system and have attracted a lot of attention in recent decades. Aerosol

Atmos. Chem. Phys. Discuss., doi:10.5194/acp-2016-1066, 2017
Manuscript under review for journal Atmos. Chem. Phys.
Published: 6 February 2017

Atmospheric Chemistry and Physics Discussions

particles suspended in the atmosphere directly influence radiative transfer of solar radiation and indirectly affect cloud properties, therefore, have large impacts on climate change. Especially, uncertainties in direct aerosol radiative forcing due to anthropogenic aerosols and in aerosol indirect forcing caused by aerosol interaction with clouds contribute most to the total uncertainty in climate forcing (Boucher et al., 2013). One of the most import factors affect these uncertainties is the interaction between aerosol particles and ambient atmospheric water vapour (Zhao et al., 2006;Kuang et al., 2016b). Under supersaturated conditions, aerosol particles serve as cloud condensation nuclei (CCN) and hence influence cloud properties. Under subsaturated conditions, with respect to typical aerosol compositions, liquid water content condensed on aerosol particles usually constitute about half of the total aerosol mass at relative humidity (RH) of 80% (Bian et al., 2014). Liquid water usually dominates the total aerosol mass in most aerosol types when RH is above 90% (Bian et al., 2014). The amounts of condensed water content in ambient aerosols and cloud droplets depend both on water uptake abilities of the aerosol components and ambient RH.

Traditionally, the Köhler theory (Petters and Kreidenweis, 2007) is widely used to describe the hygroscopic growth of aerosol particles and successfully used in laboratory studies for single component and some multicomponent particles. However, it is found that most atmospheric aerosol particles usually consist of both organic and inorganic constituents (Murphy et al., 1998) rather than consist of a single component. Given this, a modified version of Köhler theory called κ-Köhler theory is proposed by Petters and Kreidenweis (2007) and widely used in recent ten years to study the hygroscopic growth of aerosol particles. The formula of this theory is expressed as the following:

$$S = \frac{D^3 - {D_d}^3}{D^3 - {D_d}^3(1-\kappa)} \cdot \exp\left(\frac{4\sigma_{s/a} \cdot M_{water}}{R \cdot T \cdot D_p \cdot g \cdot \rho_w}\right) \quad (1)$$

where S is the saturation ratio, D is the diameter of the droplet, D_d is the dry diameter, $\sigma_{s/a}$ is the surface tension of solution/air interface, T is the temperature, M_{water} is the molecular weight of water, R is the universal gas constant, ρ_w is the density of water, and κ is the hygroscopicity parameter. This theory is not only applicable to single-component aerosol particles, but also to multicomponent aerosol particles. With regard to a multicomponent aerosol particle, the Zdanovskii, Stokes, and Robinson assumption can be applied. The hygroscopicity parameter κ of multicomponent aerosol particle can be derived by using the following formula: $\kappa = \sum_i \varepsilon_i \cdot \kappa_i$, where κ_i and ε_i represent the hygroscopic parameter and volume fraction of each component. In recent ten years, this hygroscopicity parameter κ has received much attentions and turns out to be a very effective parameter to study aerosol hygroscopicity. This hygroscopicity parameter κ makes the comparison of the aerosol hygroscopicity at different sites around the world and different time periods more convenient. In addition, hygroscopicity parameter κ also facilitates the intercomparison of aerosol hygroscopicity derived from different techniques and measurements made at different RHs. This hygroscopicity parameter κ is widely used to account the influence of aerosol hygroscopic growth on aerosol optical properties as well as aerosol liquid water contents (Tao et al., 2014;Kuang et al., 2015;Brock et al., 2016;Bian et al., 2014;Zieger et al., 2013) and to examine the role of aerosol hygroscopicty in CCN (Chen et al., 2014;Gunthe et al., 2009;Ervens et al., 2010). Therefore, the derived κ values from field campaigns and laboratory studies will further our understanding in aerosol hygroscopicity and help estimate the influences of aerosol hygroscopic growth on different aspects of atmospheric processes.

Currently, several types of instruments are widely used in field campaigns to study the aerosol hygroscopicity through different aspects of aerosol properties. The Humidity Tandem Differential mobility Analyzer (HTDMA) operates below water saturation and directly measures the aerosol hygroscopic growth factor of selected particles which have certain diameters at specified RH points. The aerosol hygroscopicity parameter κ can be directly derived from measurements of HTDMA by applying equation (1) (Liu et al., 2011;Wu et al., 2016). Through relating the aerosol hygroscopicty to CCN properties, measurements of size resolved CCN efficiency spectra can also be used to infer the hygroscopicity parameter κ at different diameters (Gunthe et al., 2009;Petters et al., 2009;Rose et al., 2010;Su et al., 2010). These two methods can both provide insights into the aerosol hygroscopicity at different aerosol diameters, however, they can only be used to derive aerosol hygroscopicity parameter κ within certain size range (usually less than 300 nm). Thus, these two methods are not capable of providing more details about aerosol hygroscopicity of aerosol particles which contribute most to aerosol optical properties and aerosol liquid water contents (their diameters usually ranging from 200 nm to 1µm) (Ma et al., 2012;Bian et al., 2014). The effect of aerosol water uptake on the aerosol particle light scattering (σ_{sp}) (sometimes aerosol extinction coefficient (Brock et al., 2016)) is usually measured with a humidified nephelometer system. Measurements from a humidified nephelometer system can also be used to calculate the aerosol hygroscopicty parameter κ if the dry aerosol particle number size distribution (PNSD) is measured simultaneously (Chen et al., 2014). The enhancement factor $f(\mathrm{RH},\lambda)$ which is defined as $f(\mathrm{RH},\lambda)=\sigma_{sp}(RH,\lambda)/\sigma_{sp}(dry,\lambda)$, is usually used as an indicator of how much the RH impacts on σ_{sp}, $\sigma_{sp}(RH,\lambda)$ or $\sigma_{sp}(dry,\lambda)$ represents σ_{sp} at wavelength λ at a certain RH or under dry conditions. In this research, $f(\mathrm{RH})$ is referred to as $f(\mathrm{RH},550\ \mathrm{nm})$ and $f(80\ \%)$ represents the $f(\mathrm{RH})$ at 80 % RH. The nephelometer measures aerosol optical properties of the entire aerosol size distribution, thus, the deduced κ value from measurements of $f(\mathrm{RH},\lambda)$ represents an overall, optically weighted κ.This κ is more suitable to be used to account the influences of aerosol hygroscopic growth on aerosol optical properties compared to aerosol hygroscopicity derived from HTDMA and CCN measurements.

Traditionally, as mentioned before, the way of deriving κ values from $f(\mathrm{RH})$ measurements require measurements of PNSD at dry state and may also need the mass concentrations of black carbon (BC) to account the influence of BC on aerosol refractive index. However, the instruments of measuring the PNSD and BC at dry state are expensive, and during field campaigns their information is sometimes not available. In this paper, with measurements from a field campaign on the North China Plain (NCP), we first derived κ values from measurements of $f(\mathrm{RH})$ with the traditional method and then compared them with the κ values derived from High Humidity Tandem Differential Mobility Analyzer (HH-TDMA). HH-TDMA is a system very similar with HTDMA but is capable of operating at higher RH points (Liu et al., 2011). The relationships between κ values derived from $f(\mathrm{RH})$ measurements and parameters used to fit measured $f(\mathrm{RH})$ curves are further examined and analyzed. Finally, basing on finished analysis about the relationship between κ and $f(\mathrm{RH})$ fitting parameters, a novel method to directly derive the aerosol hygroscopicity parameter κ based only on measurements from a humidified nephelometer system is proposed. This newly proposed approach makes it more convenient and cheaper for researchers to conduct aerosol hygroscopicity research with measurements of $f(\mathrm{RH})$.

2. Site description and instruments

In this study, the main part of used datasets is from the field campaign conducted at Wangdu ($38°40'N, 115°08'$E) during summer on the North China Plain (NCP). This field campaign was jointly conducted by Peking University, China and Leibniz-Institute for Tropospheric Research, Germany. Wangdu site is located in the suburban district of Wangdu County, Hebei Province, China and situated adjacent to farmland and residential areas, it belongs to the typical region of the NCP. This observation campaign lasted for about one month from 4 June, 2014 to 14 July, 2014. The measured $f(\mathrm{RH},\lambda)$

dataset was available from June 21st, 2014, to July 1st, 2014.

For datasets from Wangdu campaign. The chemical compositions of the aerosol particles with an aerodynamic diameter of less than 2.5 μm (PM2.5) were analyzed based on the samples collected on quartz and Teflon filters. Other instruments share one inlet which is placed on the roof of the container. Regarding this inlet system, aerosol particles first entered an impactor which selected the aerosol particles with an aerodynamic diameter of less than 10 μm, and then passed through a dryer which is capable of reducing the RH of the sample air to lower than 30 %. In succession, the sample air passed through a splitter and was allotted to different instruments according to their required flow rates. The PNSD at dry state ranging from 3nm to 10μm was observed jointly by a Twin Differential Mobility Particle Sizer (TDMPS, Leibniz-Institute for Tropospheric Research (IfT), Germany; Birmili et al. (1999)) and an Aerodynamic Particle Sizer (APS, TSI Inc., Model 3321) with a temporal resolution of 10 minutes. The absorption coefficient at 637 nm was measured using a Multi-angle Absorption Photometer (MAAP Model 5012, Thermo, Inc., Waltham, MA USA) with a temporal resolution of 1 minute, and further used to calculate the mass concentrations of black carbon (BC) with a constant mass absorption efficiency (MAE) of 6.6 m^2g^{-1}. The growth factors of aerosol particles at six selected particle diameters (30 nm, 50 nm, 100 nm, 150nm, 200 nm and 250 nm) at 98% RH condition were obtained from the measurements of the HH-TDMA (Leibniz-Institute for Tropospheric Research (IfT), Germany; Hennig et al. (2005)). The $f(\mathrm{RH},\lambda)$ curves of aerosol particles with RH ranging from about 50% to 90% were measured by a humidified nephelometer system which consists of two three-wavelength integrating nephelometers (TSI Inc., Model 3563) and a humidifier. The humidifier was used to moisten the air which will be sampled into the second nephelometer. Details of this humidified nephelometer system please refer to (Kuang et al., 2016a).

PNSDs at dry state and mass concentrations of BC derived from MAAP measurements measured at both Wuqing from 12 July to 14 August in 2009 and Xianghe from 9 July to 8 August in 2013 are also used in this study to examine the influence of PNSD and BC on derivation of κ values from $f(\mathrm{RH})$ measurements and other relationships. Additionally, σ_{sp} values which were observed during these three field campaigns introduced before with a three-wavelength integrating nephelometer (TSI Inc., Model 3563) are also used in Sect.4.3. Both Wuqing and Xianghe are representative regional background sites of the NCP and locates in the northern part of the NCP. Details about these two campaigns can be found in papers published by Kuang et al. (2015) and Ma et al. (2016).

Atmos. Chem. Phys. Discuss., doi:10.5194/acp-2016-1066, 2017
Manuscript under review for journal Atmos. Chem. Phys.
Published: 6 February 2017

3. Methodology

3.1 Calculations of hygroscopicity parameter κ from measurements of $f(\mathrm{RH})$ and HH-TDMA

Research of Chen et al. (2014) demonstrated that if the PNSD at dry state is measured, then measurements of $f(\mathrm{RH})$ can be used to derive the aerosol hygroscopicity parameter κ by conducting an iterative calculation with the Mie theory and the κ-Köhler theory. To reduce the influence of random errors of observed $f(\mathrm{RH})$ at a certain RH, all valid $f(\mathrm{RH})$ measurements in a complete humidifying cycle is used in the derivation algorithm. The retrieved κ is the κ value which can be used to best fit the observed $f(\mathrm{RH})$ curve. Details about this retrieval algorithm is described in Chen et al. (2014). Of particular note is that in this research the mass concentration of BC is also considered in the retrieval algorithm to account for the influence of BC on refractive indices of aerosol particles at different sizes. The BC is considered to be homogeneously mixed with other aerosol components, and the mass size distribution of BC used in Ma et al. (2012) which is observed on the NCP is used in this research to account the mass distributions of BC at different particle sizes. The used refractive index and density of BC are $1.80 - 0.54\mathrm{i}$ and $1.5\mathrm{g}\ cm^{-3}$ (Kuang et al., 2015). Used refractive indices of non light-absorbing aerosol components (other than BC) and liquid water are $1.53 - 10^{-7}i$ (Wex et al., 2002) and $1.33 - 10^{-7}i$ (Seinfeld and Pandis, 2006), respectively.

The HH-TDMA measures hygroscopic growth factors of particles at different sizes at 98% RH condition. The measured hygroscopic factors can be directly related to κ with equation (1). For a specified size of selected aerosol particles, a distribution of growth factors can be measured, and thus can be used to derive a probability distribution of κ and finally come to the calculation of average κ value corresponding to this size of aerosol particles. The method on how to derive average κ value of certain size of aerosol particles from HH-TDMA measurements is elaborately described in Liu et al. (2011).

3.2 Parameterization schemes for $f(\mathrm{RH})$

Due to the complex chemical compositions of ambient aerosol particles and the challenge in precisely measuring their molecular compositions, it is difficult to directly describe the influence of RH on σ_{sp}. Some simplified parameterization schemes are usually used to describe $f(\mathrm{RH})$ as a function of RH. The most frequently used parameterization scheme is a power-law function which is known as "gamma" parameterization (Quinn et al., 2005) and the formula of this single-parameter representation is written as the following:

Atmos. Chem. Phys. Discuss., doi:10.5194/acp-2016-1066, 2017
Manuscript under review for journal Atmos. Chem. Phys.
Published: 6 February 2017

Atmospheric Chemistry and Physics Discussions

$$f(\mathrm{RH}) = \left[\frac{(100-RH_0)}{100-RH}\right]^{\gamma} \quad (2)$$

where RH_0 is the RH of dry condition, and γ is a parameter fitted to the observed $f(\mathrm{RH})$. In this study, we estimated γ values with observed $f(\mathrm{RH})$ curves and for the first time to our knowledge, we further examined the relationship between γ and κ retrieved from $f(\mathrm{RH})$ measurements.

Recently, a new physically based single-parameter representation was proposed by Brock et al. (2016) to describe $f(\mathrm{RH})$. Their results demonstrated that this proposed parameterization scheme can better describe $f(\mathrm{RH})$ than the widely used gamma power-law approximation (Brock et al., 2016). The formula of this new scheme is written as:

$$f(\mathrm{RH}) = 1 + \kappa_{sca}\frac{RH}{100-RH} \quad (3)$$

where κ_{sca} is a parameter fitted to observed $f(\mathrm{RH})$. Here, we give a brief introduction about the physical understanding of this alternative parameterization scheme. Regardless of the curvature effects for particle diameters larger than 100 nm, the hygroscopic growth factor for aerosol particles can be approximately expressed as the following (Brock et al., 2016): $gf_{diam} \cong (1 + \kappa\frac{RH}{100-RH})^{1/3}$. Moreover, σ_{sp} is usually proportional to total aerosol volume (Pinnick et al., 1980) which means that the relative change in σ_{sp} due to aerosol water uptake is roughly proportional to relative change in aerosol volume. The enhancement factor in volume can be expressed as the cube of gf_{diam}, thus lead to the formula form of $f(\mathrm{RH})$ expressed in equation (3). More details about the discussion of this new expression form of $f(\mathrm{RH})$ can be found in the paper published by Brock et al. (2016). In this paper, the performance of this newly proposed scheme is investigated, values of κ_{sca} are estimated from observed $f(\mathrm{RH})$ curves and their relationship with κ values retrieved from $f(\mathrm{RH})$ measurements is also examined.

These two parameterization schemes which are introduced here are referred to as γ-Method and κ_{sca}-Method respectively in the following paragraphs.

4. Results and discussions

4.1 Derived κ values from $f(\mathrm{RH})$ and HH-TDMA measurements

During this field campaign, the aerosol physical, chemical and optical properties are synergistically observed with different types of instruments. They provide valuable datasets to perform an insightful analysis about aerosol hygroscopicity and its relationship with other aerosol properties.

The time series of σ_{sp} at 550 nm at dry state are shown in Fig.1a, and values of σ_{sp} at 550 nm shown in Fig.1a are corrected from measurements of TSI 3563 nephelometer (the truncation errors are corrected using Mie theory with measured PNSD and mass concentrations of BC). The results show that this observation period has experienced varying degrees of pollution levels, with σ_{sp} at 550 nm ranging from 15 to 1150 Mm^{-1}. The aerosol chemical compositions also change a lot during the observation period. The relative contributions of mass concentrations of organic matter to total PM2.5 mass concentrations range from 2% to 42%. Moreover, the relative contributions of mass concentrations of sulfate, nitrate and ammonium to total PM2.5 mass concentrations range from 5 to 50 %, 2 to 27 % and 1 to 21 %, respectively (Kuang et al., 2016a). These results imply that during this observation period, the aerosol hygroscopicity changes a lot whereafter corroborated by $f(\mathrm{RH})$ measurements. Overall, $f(80\ \%)$ values range between 1.1 and 2.3 with an average of 1.8. Periods when deliquescent phenomena occur, $f(80\ \%)$ values are relatively higher with a variation range of 1.7 to 2.3 and their average is 2.0. This is because of the dominance of ammonium sulfate during periods when deliquescent phenomena occur. More detailed analysis about the frequently observed deliquescent phenomena during this field campaign please refer to (Kuang et al., 2016a).

Furthermore, κ values derived from $f(\mathrm{RH})$ measurements by combining measurements of PNSD at dry state and mass concentrations of BC are shown in Fig.1b. During deliquescent phenomena periods, $f(\mathrm{RH})$ jumps when sample RH in the cavity of the nephelometer mainly ranges from 60 % to 65 %. Therefore, for a humidifying cycle which shows jump phenomenon in $f(\mathrm{RH})$, only $f(\mathrm{RH})$ points when RHs are greater than 70% (after the jump point) are used to retrieve κ. The results demonstrate that κ derived from $f(\mathrm{RH})$ measurements (hereinafter referred to as $\kappa_{f(\mathrm{RH})}$) lie between 0.06 and 0.43. The lowest $\kappa_{f(\mathrm{RH})}$ values are found when the air quality is relatively clean (σ_{sp} at 550 nm is lower than 100 Mm^{-1}) on 27 and 28 June. During these two days, organic matter dominates the mass concentration of PM2.5 which results in the low hygroscopicity of aerosol particles. On the contrary, the largest $\kappa_{f(\mathrm{RH})}$ values are found during periods when deliquescent phenomena occur and inorganic chemical compositions dominate the mass concentrations of PM2.5, especially, sulfate is highly abundant during these periods. Of particular note is that during relatively polluted periods (σ_{sp} at 550 nm larger than 100 Mm^{-1}) aerosol particles are generally very hygroscopic which imply that aerosol water uptake can exert significant impacts on regional direct aerosol radiative effect

Atmos. Chem. Phys. Discuss., doi:10.5194/acp-2016-1066, 2017
Manuscript under review for journal Atmos. Chem. Phys.
Published: 6 February 2017

and ambient visibility during this observation period. On the whole, the average $\kappa_{f(\mathrm{RH})}$ during this observation period is 0.28.

On the basis of the average size-resolved κ distribution from Haze in China (HaChi) campaign (Liu et al., 2014), κ values change a lot for aerosol particles whose diameters are less than 250 nm, however, κ values vary relatively smaller for aerosol particles whose diameter range from 250 nm to 1 μm. In addition, the results from HaChi campaign also demonstrate that aerosol particles whose diameter range from 200 nm to 1 μm usually contribute more than 80% to σ_{sp} at 550 nm during summer on the NCP (Ma et al., 2012). To compare κ values derived from measurements of humidified nephelometer system and HH-TDMA, average κ values corresponding to aerosol particles at only 250 nm which are derived from HH-TDMA measurements are also shown in Fig.1b. In the following, average κ which is derived from HH-TDMA measurements for aerosol particles having particle size of 250 nm is referred to as κ_{250}. During this observation period, values of κ_{250} range from 0.11 to 0.56, with an average of 0.34 which is very close to average κ_{250} observed during HaChi campaign (Liu et al., 2011). The results shown in Fig.1b suggest that, in general, $\kappa_{f(\mathrm{RH})}$ values agree well with κ_{250} values, however, are usually lower than κ_{250} values. To quantitatively compare these two types of κ values, they are plotted against each other and shown in Fig.2. It can be seen that they are highly correlated but the κ_{250} values are systematically higher than $\kappa_{f(\mathrm{RH})}$ values, and the average difference between κ_{250} and $\kappa_{f(\mathrm{RH})}$ is 0.06. The statistical relationship between κ_{250} and $\kappa_{f(\mathrm{RH})}$ is also shown in Fig.2.This relationship may be useful for researchers if they want to estimate the influences of aerosol water uptake on aerosol optical properties and aerosol liquid water contents when only HH-TDMA or HTDMA measurements are available.

A model experiment is conducted to better understand the relationship between κ_{250} and $\kappa_{f(\mathrm{RH})}$. During HaChi campaign, size-resolved κ distributions are derived from measured size-segregated chemical compositions (Liu et al., 2014) and their average is used in this experiment to account the size dependence of aerosol hygroscopicity which is shown in Fig. 3a. With this fixed average size-resolved κ distribution, all observed PNSDs at dry state along with mass concentrations of BC whicih are observed at three different representative background sites of the NCP during summer are used to simulate the retrieval of $\kappa_{f(\mathrm{RH})}$ under different PNSD and BC conditions. Field campaigns conducted at these three site is introduced in Sect.2. The treatment of BC is the same with the way in the process of deriving $\kappa_{f(\mathrm{RH})}$ which is introduced in Sect.4.1. The used PNSDs shown in Fig.3b show that large varying types of PNSDs are considered in the simulative experiment. The probability distribution of simulated $\kappa_{f(\mathrm{RH})}$ is also shown in Fig.3a. The standard deviation of retrieved $\kappa_{f(\mathrm{RH})}$ is about 0.01 which suggests that if the size-resolved κ distribution is fixed, then $\kappa_{f(\mathrm{RH})}$ varies little. Due to $\kappa_{f(\mathrm{RH})}$ represents an overall, optically weighted κ, it is clearly shown in Fig.3a that in most cases $\kappa_{f(\mathrm{RH})}$ values are located between κ values of aerosol particles ranging from 200 nm to 1 μm. Moreover, about 70% of simulated $\kappa_{f(\mathrm{RH})}$ values are less than κ_{250} which to some extent explains the observed difference between κ_{250} and $\kappa_{f(\mathrm{RH})}$ mentioned before. However, the simulated average difference between κ_{250} and average $\kappa_{f(\mathrm{RH})}$ is about 0.01 which is far less than the observed averaged difference between κ_{250} and $\kappa_{f(\mathrm{RH})}$ which is 0.06. Except that uncertainties from measurements of instruments, for example, the uncertainty of RH in measurements of HH-TDMA and uncertainties of measuring $f(\mathrm{RH})$ (details about the uncertainty sources of $f(\mathrm{RH})$ measurements can be found in the paper published by Titos et al. (2016)), there are other two reasons may be associated with this discrepancy. The first one is that configurations of size-resolved κ distributions and PNSDs during this field campaign are far different from the model experiment. The second one is that in the real atmosphere, κ values at different RH conditions may be different (You et al., 2014) and most of $f(\mathrm{RH})$ measurements are conducted when RH is lower than 90%, however, the measurements of HH-TDMA are conducted when RH is equal to 98% . Overall, the observed general consistency between κ values derived from measurements of $f(\mathrm{RH})$ and HH-TDMA confirms the reliability of κ values derived from $f(\mathrm{RH})$ measurements.

4.2 Relationships between κ derived from $f(\mathrm{RH})$ measurements and $f(\mathrm{RH})$ fitting parameters

In the previous section, the overall properties of ambient aerosol particles are introduced, derived $\kappa_{f(\mathrm{RH})}$ values are characterized and compared with κ_{250} values. These results demonstrated that derived $\kappa_{f(\mathrm{RH})}$ values can commendably represent variations of aerosol hygroscopicty of ambient aerosol populations. In this section, the relationship between derived $\kappa_{f(\mathrm{RH})}$ values and $f(\mathrm{RH})$ fitting parameters are further examined to investigate their relationships.

Two parameterization schemes of $f(\mathrm{RH})$ are discussed in this paper, including the currently widely used γ-Method and newly proposed κ_{sca}-Method by Brock et al. (2016) and both methods are introduced in Sect.3.2. A fitting example of these two methods is shown in Fig.4A. For $f(\mathrm{RH})$

cycles observed during this field campaign, they are fitted by using both γ-Method and κ_{sca}-Method, corresponding values of γ and κ_{sca} are also deduced. For cycles during deliquescent periods, only $f(\mathrm{RH})$ points with RH higher than 70% are used to perform fitting processes. The fitting performance of these two methods are further investigated by conducting the comparison between measured and fitted $f(85)\%$ values. Probability distributions of the ratio between fitted and measured $f(85)\%$ by using these two methods are shown in Fig.4B. The results indicate that in most cases both γ-Method and κ_{sca}-Method fit observed $f(\mathrm{RH})$ cycles well with γ-Method performs slightly better which is contrary to the results introduced by Brock et al. (2016), their results demonstrate that κ_{sca}-Method can better describe observed $f(\mathrm{RH})$ than γ-Method. That is to say, $f(\mathrm{RH})$ curves observed at different places or time periods may require different parameterization schemes to fit them best, however, in general both γ-Method and κ_{sca}-Method are good approaches to fit observed $f(\mathrm{RH})$ curves.

Concerning γ-Method, previous studies usually examine the relationship between γ and aerosol chemical compositions and established several parameterization schemes to fit γ with mass fractions of different aerosol chemical compositions, including organic materials, sulfate and nitrate (Quinn et al., 2005;Titos et al., 2014;Zhang et al., 2015). However, to obtain a reliable estimation of γ, complete information of aerosol chemical compositions may be required which is difficult to get, and it is also hard to find a comprehensive description of γ based on those complicated chemical compositions. Single aerosol hygroscopicity parameter κ can represent overall hygroscopicity of aerosol particles which contains influences of different chemical compositions on aerosol hygroscopicity, therefore may be used to better fit γ. In view of this, the relationship between $\kappa_{f(\mathrm{RH})}$ and γ is investigated and shown in Fig.4C. It is found that a pretty good linear relationship exists (square of correlation coefficient is 0.95) between $\kappa_{f(\mathrm{RH})}$ and γ, especially when $\kappa_{f(\mathrm{RH})}$ is larger than 0.15. This correlation is far better than previously found relationships between γ and aerosol chemical compositions (Quinn et al., 2005;Titos et al., 2014;Zhang et al., 2015) and statistical parameters which can be used to parameterize γ with $\kappa_{f(\mathrm{RH})}$ is also shown in Fig.4C. During this field campaign, fitted γ ranges from 0.15 to 0.63 with an average of 0.46.

Furthermore, during this field campaign, fitted κ_{sca} ranges from 0.05 to 0.3 with an average of 0.2. The relationship between $\kappa_{f(\mathrm{RH})}$ and κ_{sca} is also investigated and it is found a strong linear relationship also exists (square of correlation coefficient is 0.98) between $\kappa_{f(\mathrm{RH})}$ and κ_{sca}. This linear relationship is even better than the linear relationship between $\kappa_{f(\mathrm{RH})}$ and γ. Not only that, the statistically fitted line almost passes though zero point which implies that a proportional relationship may exist between $\kappa_{f(\mathrm{RH})}$ and κ_{sca}. This strong correlation should be intrinsic due to the idea of κ_{sca}-Method is from the linkage between total aerosol volume and σ_{sp} as introduced in Sect.3.2 and the increase of total aerosol volume due to aerosol water uptake is directly linked to the overall aerosol hygroscopicity parameter κ. It seems that this promising linear relationship can help bridge the gap between $f(\mathrm{RH})$ and κ. However, results from Brock et al. (2016) demonstrated that the relationship between $\kappa_{f(\mathrm{RH})}$ and κ_{sca} is much more sophisticated and it is affected by both aerosol hygroscopicity and PNSD at dry state. In the paper published by Brock et al. (2016), κ_{ext} and κ_{chem} are used and correspond to κ_{sca} and $\kappa_{f(\mathrm{RH})}$ in this research, the difference between κ_{ext} and κ_{sca} is that κ_{ext} is used to fit the light enhancement factor of aerosol extinction coefficient, κ_{chem} and $\kappa_{f(\mathrm{RH})}$ actually means the same because both them are overall and size independent hygroscopicity parameters. Results from Brock et al. (2016) concluded that the ratio $\kappa_{ext}/\kappa_{chem}$ generally lies between 0.6 to 1 which implies that the ratio $\kappa_{sca}/\kappa_{f(\mathrm{RH})}$ (in the following, this ratio is referred to as R_κ) also should have large variations and shares the similar variation range. By revisiting the relationship between $\kappa_{f(\mathrm{RH})}$ and κ_{sca} found in this research, it can be found that R_κ during this field campaign ranges from 0.6 to 0.77 with an average of 0.7. This result suggests that if we directly establish a linkage between $\kappa_{f(\mathrm{RH})}$ and κ_{sca} with an average R_κ can result in a non-negligible bias (relative difference can reach about 15%). Besides, this range of R_κ only represents the relationship between $\kappa_{f(\mathrm{RH})}$ and κ_{sca} during a short time period and at only one site.

To better understand the relationship between $\kappa_{f(\mathrm{RH})}$ and κ_{sca}, all PNSDs at dry state (shown in Fig.3a) along with mass concentrations of BC observed from three different representative background sites of the NCP during summer which is introduced in Sect.2 are used to simulate the relationship between $\kappa_{f(\mathrm{RH})}$ and κ_{sca} with Mie and κ-Köhler theories. During simulating processes, for each PNSD, we change $\kappa_{f(\mathrm{RH})}$ from 0.01 to 0.6 with an interval of 0.01 to examine the influence of aerosol hygroscopicity on R_κ. The way of treating BC is same with the simulation experiment introduced in Sect.4.1. Simulated results are shown in Fig.5a and the probability distribution of simulated R_κ values is shown in Fig.5b. The results show that R_κ primarily ranges from 0.55 to 0.82 with an average of 0.69 which is very close to the average R_κ measured during the field campaign of

Atmos. Chem. Phys. Discuss., doi:10.5194/acp-2016-1066, 2017
Manuscript under review for journal Atmos. Chem. Phys.
Published: 6 February 2017

this research. These results also indicate that the relationship between $\kappa_{f(\mathrm{RH})}$ and κ_{sca} is much more complex than a simple linear relationship and more information about aerosol properties are necessary to gain insights into the variation of R_κ.

4.3 A novel method to directly derive κ from measurements of a humidified nephelometer system

A robust linear relationship is first found between $\kappa_{f(\mathrm{RH})}$ and κ_{sca} in Sect.4.2 and then it turns out that the relationship between $\kappa_{f(\mathrm{RH})}$ and κ_{sca} is much more complex than that shown in Fig.4D. The complexity comes from large variations of R_κ and both PNSD at dry state and aerosol hygroscopicity have impacts on R_κ. Generally, used nephelometer of a humidified nephelometer system have three wavelengths (Titos et al., 2016) and the spectral dependence of σ_{sp} is usually described by the following Ångström formula: $\sigma_{sp}(\lambda) = \beta\lambda^{-\alpha_{sp}}$, where β is the particle number concentration dependent coefficient, λ is the wavelength of light and α_{sp} represents the Ångström exponent of σ_{sp} (Zieger et al., 2014). Thus, Ångström exponent can be directly inferred from the measurements of σ_{sp} at different wavelengths. Of particular note is that Ångström exponent can not only be used to account the spectral course of σ_{sp}, it also reveals information about PNSD. In general, larger value of Ångström exponent corresponds to smaller aerosol particles. That is, Ångström exponent can be a proxy of PNSD at dry state and be used in the processes of estimating the impacts of PNSD on R_κ. On the other hand, with regard to aerosol hygroscopicity, although R_κ varies within certain range, value of κ_{sca} can still be used to represent the overall hygroscopicity of aerosol particles. Given this, simulated R_κ values introduced in the last paragraph of Sect.4.2 are spread into a two dimensional gridded plot. The first dimension is Ångström exponent with an interval of 0.02 and the second dimension is κ_{sca} with an interval of 0.01, average R_κ value within each grid is represented by color and shown in Fig.6a. Values of Ångström exponent corresponding different PNSDs are calculated from concurrently measured σ_{sp} values at 450 nm and 550 nm from TSI 3563 nephelometer. Basing on results shown on Fig.6a, the different impacts of aerosol hygroscopicity and PNSD at dry state on R_κ can be clearly distinguished. The results demonstrate that PNSD at dry state dominates the variation of R_κ, nevertheless, aerosol hygroscopicty has non-negligible impacts. Overall, larger value of Ångström exponent corresponds to higher R_κ. However, aerosol hygroscopicty exhibits different influences on R_κ when Ångström exponent values are different. Generally speaking, higher κ_{sca} corresponds to lower R_κ if Ångström exponent is smaller than about 0.8 and higher κ_{sca} corresponds to higher R_κ if Ångström exponent is larger than about 1.6.

In addition, the percentile value of standard deviation of R_κ values within each grid divided by their average is shown in Fig.6b. In most cases, these percentile values are less than 6% (about 90%) which demonstrates that R_κ varies little within each grid shown in Fig.6a. This implies that results of Fig.6a can be used as a look up table to estimate R_κ. As what's introduced before, currently widely used nephelometer of a humidified nephelometer system usually have three wavelengths (Titos et al., 2016), thus can provide information about Ångström exponent, and κ_{sca} can be directly fitted from observed $f(\mathrm{RH})$ curve. Even only one $f(\mathrm{RH})$ point is measured κ_{sca} can still be calculated from equation (3). Therefore, using results shown in Fig.6a as a look up table, R_κ values can be directly predicted from measurements of a humidified nephelometer system. With this method, R_κ values during this Wangdu field campaign are predicted (values of Ångström exponent are calculated from measured σ_{sp} values at 450 nm and 550 nm under dry conditions) and compared with measured R_κ values, the results are shown in Fig.7a. The Ångström exponent during this field campaign ranges from 0.63 to 1.96 with an average of 1.4. It can be seen from Fig.7a that majority of points lie nearby 1:1 line and 92% points have relative differences less than 6% which is consistent with results shown in Fig.6b. This result is quite promising and can be further used to derive $\kappa_{f(\mathrm{RH})}$ values by combining fitted κ_{sca} and predicted R_κ. The results of predicted $\kappa_{f(\mathrm{RH})}$ values are shown in Fig.7b and a robust correlation between predicted $\kappa_{f(\mathrm{RH})}$ values and $\kappa_{f(\mathrm{RH})}$ values retrieved by using the traditional method introduced in Sect.3.1 is achieved (square of correlation coefficient is 0.99). All points shown in Fig.7b lie nearby 1:1 line, average difference between $\kappa_{f(\mathrm{RH})}$ derived from newly proposed method and traditional method is -0.005. This result demonstrates a quite good estimation of $\kappa_{f(\mathrm{RH})}$ can be achieved by using only measurements from a humidified nephelometer system.

It should be noted that the look up table shown in Fig.6a already covers large variation ranges of Ångström exponent and κ_{sca}. Which means that this look up table can be used under different conditions. However, it should be pointed out that the look up table shown in Fig.6a is from simulations of measured continental aerosols without influences of desert dust, and it might not be suitable for

Atmos. Chem. Phys. Discuss., doi:10.5194/acp-2016-1066, 2017
Manuscript under review for journal Atmos. Chem. Phys.
Published: 6 February 2017

being used to estimate $\kappa_{f(\mathrm{RH})}$ when sea salt or dust particles prevail. In summary, this approach allows researchers to directly derive aerosol hygroscopicity from measurements of $f(\mathrm{RH})$ without any additional information about PNSD and BC which is quite convenient for researchers to conduct aerosol hygroscopicity researches with measurements from a humidified nephelometer system.

5. Conclusions

During the field campaign introduced in this paper, which is conducted in summer at a background site of the NCP, integrative aerosol information including aerosol chemical, optical and physical properties are observed. Among them, aerosol hygroscopicty is crucial for understanding roles of aerosol particles in air pollution and aerosol climate effects. In this paper, values of aerosol hygroscopicity parameter κ are first derived from measurements of $f(\mathrm{RH})$ by combining measurements of PNSD at dry state and BC. The results show that during this field campaign, aerosol hygroscopicity varies a lot, and $\kappa_{f(\mathrm{RH})}$ ranges from 0.06 to 0.43 with an average of 0.28. Retrieved $\kappa_{f(\mathrm{RH})}$ values are further compared with κ_{250} which is derived from measurements of HH-TDMA and good consistency is achieved. Results show that κ_{250} is systematically higher than $\kappa_{f(\mathrm{RH})}$ and the average of their difference is 0.06. A simulative experiment is conducted to better understand their difference and partially explained the observed discrepancy, however, still not enough and possible reasons are discussed in Sect.4.1.

Relationships between $\kappa_{f(\mathrm{RH})}$ and $f(\mathrm{RH})$ fitting parameters γ and κ_{sca} are further investigated in Sect.4.2 which is for the first time to our knowledge. Good linear relationship exists between $\kappa_{f(\mathrm{RH})}$ and γ, and the correlation between $\kappa_{f(\mathrm{RH})}$ and γ is far better than previously found relationships between γ and aerosol chemical compositions. This results demonstrate that κ should be a better choice to parameterize $f(\mathrm{RH})$ fitting parameters than mass fractions of aerosol chemical compositions which is so far widely used. The relationship between $\kappa_{f(\mathrm{RH})}$ and κ_{sca} is then also examined, and it is found that a better linear relationship than the relationship between $\kappa_{f(\mathrm{RH})}$ and γ exists between $\kappa_{f(\mathrm{RH})}$ and κ_{sca}, and $\kappa_{f(\mathrm{RH})}$ may be proportional to κ_{sca}. However, through detailed analysis about the relationship between $\kappa_{f(\mathrm{RH})}$ and κ_{sca}, it turns out that their relationship is more complicated than what is found at the very beginning and the ratio $\kappa_{sca}/\kappa_{f(\mathrm{RH})}$ (R_{κ}) varies a lot. Results show that both PNSD at dry state and aerosol hygroscopicity have impacts on value of R_{κ}.

In Sect.4.3, by introducing Ångström exponent as a proxy for PNSD, impacts of PNSD and aerosol hygroscopicity on R_{κ} are distinguished and then discussed. In succession, a look up table based on Ångström exponent and κ_{sca} is developed to estiamte R_κ. With this look up table, R_κ can be directly estimated from measurements of a humidified nephelometer system. This method is further verified with measurements of this field campaign. Results show that great consistency is achieved between predicted and measured R_κ values (92% points have relative difference less than 6%). Given this, the linkage between $\kappa_{f(\mathrm{RH})}$ and κ_{sca} is directly established and further used to estimate $\kappa_{f(\mathrm{RH})}$. The comparison results demonstrate a pretty good agreement is achieved, all points lie nearby 1:1 line. The average absolute difference between $\kappa_{f(\mathrm{RH})}$ derived from newly proposed method and traditional method is -0.005 and the square of correlation coefficient between them is 0.99. This newly proposed novel approach allow researchers to estimate $\kappa_{f(\mathrm{RH})}$ without any additional information about PNSD and BC. This new finding directly links κ and $f(\mathrm{RH})$ and will make the humidified nephelometer system more convenient when it comes to aerosol hygroscopicity research. Finally, findings in this research may facilitate the intercomparison of aerosol hygroscopicity derived from different techniques, help for parameterizing $f(\mathrm{RH})$ and predicting CCN properties with optical measurements.

Acknowledgments

This work is supported by the National Natural Science Foundation of China (41590872, 41375134). The data used are listed in the references and a repository at http://pan.baidu.com/s/1c2Nzc5a.

References

Bian, Y. X., Zhao, C. S., Ma, N., Chen, J., and Xu, W. Y.: A study of aerosol liquid water content based on hygroscopicity measurements at high relative humidity in the North China Plain, Atmos. Chem. Phys., 14, 6417-6426, 10.5194/acp-14-6417-2014, 2014.

Birmili, W., Stratmann, F., and Wiedensohler, A.: Design of a DMA-based size spectrometer for a large particle size range and stable operation, Journal of Aerosol Science, 30, 549-553, 10.1016/s0021-8502(98)00047-0, 1999.

Boucher, O., Randall, D., Artaxo, P., Bretherton, C., Feingold, G., Forster, P., Kerminen, V.-M., Kondo, Y., Liao, H., Lohmann, U., Rasch, P., Satheesh, S. K., Sherwood, S., Stevens, B., and Zhang, X. Y.: Clouds and Aerosols, in: Climate Change 2013: The Physical Science Basis. Contribution of Working Group I to the Fifth Assessment Report of the Intergovernmental

Atmos. Chem. Phys. Discuss., doi:10.5194/acp-2016-1066, 2017
Manuscript under review for journal Atmos. Chem. Phys.
Published: 6 February 2017

Atmospheric Chemistry and Physics Discussions
Open Access

Panel on Climate Change, edited by: Stocker, T. F., Qin, D., Plattner, G.-K., Tignor, M., Allen, S. K., Boschung, J., Nauels, A., Xia, Y., Bex, V., and Midgley, P. M., Cambridge University Press, Cambridge, United Kingdom and New York, NY, USA, 571–658, 2013.

Brock, C. A., Wagner, N. L., Anderson, B. E., Attwood, A. R., Beyersdorf, A., Campuzano-Jost, P., Carlton, A. G., Day, D. A., Diskin, G. S., Gordon, T. D., Jimenez, J. L., Lack, D. A., Liao, J., Markovic, M. Z., Middlebrook, A. M., Ng, N. L., Perring, A. E., Richardson, M. S., Schwarz, J. P., Washenfelder, R. A., Welti, A., Xu, L., Ziemba, L. D., and Murphy, D. M.: Aerosol optical properties in the southeastern United States in summer – Part 1: Hygroscopic growth, Atmos. Chem. Phys., 16, 4987-5007, 10.5194/acp-16-4987-2016, 2016.

Chen, J., Zhao, C. S., Ma, N., and Yan, P.: Aerosol hygroscopicity parameter derived from the light scattering enhancement factor measurements in the North China Plain, Atmos. Chem. Phys., 14, 8105-8118, 10.5194/acp-14-8105-2014, 2014.

Ervens, B., Cubison, M. J., Andrews, E., Feingold, G., Ogren, J. A., Jimenez, J. L., Quinn, P. K., Bates, T. S., Wang, J., Zhang, Q., Coe, H., Flynn, M., and Allan, J. D.: CCN predictions using simplified assumptions of organic aerosol composition and mixing state: a synthesis from six different locations, Atmos. Chem. Phys., 10, 4795-4807, 10.5194/acp-10-4795-2010, 2010.

Gunthe, S. S., King, S. M., Rose, D., Chen, Q., Roldin, P., Farmer, D. K., Jimenez, J. L., Artaxo, P., Andreae, M. O., Martin, S. T., and Pöschl, U.: Cloud condensation nuclei in pristine tropical rainforest air of Amazonia: size-resolved measurements and modeling of atmospheric aerosol composition and CCN activity, Atmos. Chem. Phys., 9, 7551-7575, 10.5194/acp-9-7551-2009, 2009.

Hennig, T., Massling, A., Brechtel, F. J., and Wiedensohler, A.: A tandem DMA for highly temperature-stabilized hygroscopic particle growth measurements between 90% and 98% relative humidity, Journal of Aerosol Science, 36, 1210-1223, 10.1016/j.jaerosci.2005.01.005, 2005.

Kuang, Y., Zhao, C. S., Tao, J. C., and Ma, N.: Diurnal variations of aerosol optical properties in the North China Plain and their influences on the estimates of direct aerosol radiative effect, Atmos. Chem. Phys., 15, 5761-5772, 10.5194/acp-15-5761-2015, 2015.

Kuang, Y., Zhao, C. S., Ma, N., Liu, H. J., Bian, Y. X., Tao, J. C., and Hu, M.: Deliquescent phenomena of ambient aerosols on the North China Plain, Geophys. Res. Lett., n/a-n/a, 10.1002/2016GL070273, 2016a.

Kuang, Y., Zhao, C. S., Tao, J. C., Bian, Y. X., and Ma, N.: Impact of aerosol hygroscopic growth on the direct aerosol radiative effect in summer on North China Plain, Atmospheric Environment, 147, 224-233, http://dx.doi.org/10.1016/j.atmosenv.2016.10.013, 2016b.

Liu, H. J., Zhao, C. S., Nekat, B., Ma, N., Wiedensohler, A., van Pinxteren, D., Spindler, G., Müller, K., and Herrmann, H.: Aerosol hygroscopicity derived from size-segregated chemical composition and its parameterization in the North China Plain, Atmos. Chem. Phys., 14, 2525-2539, 10.5194/acp-14-2525-2014, 2014.

Liu, P. F., Zhao, C. S., Göbel, T., Hallbauer, E., Nowak, A., Ran, L., Xu, W. Y., Deng, Z. Z., Ma, N., Mildenberger, K., Henning, S., Stratmann, F., and Wiedensohler, A.: Hygroscopic properties of aerosol particles at high relative humidity and their diurnal variations in the North China Plain, Atmos. Chem. Phys., 11, 3479-3494, 10.5194/acp-11-3479-2011, 2011.

Ma, N., Zhao, C. S., Müller, T., Cheng, Y. F., Liu, P. F., Deng, Z. Z., Xu, W. Y., Ran, L., Nekat, B., van Pinxteren, D., Gnauk, T., Müller, K., Herrmann, H., Yan, P., Zhou, X. J., and Wiedensohler, A.: A new method to determine the mixing state of light absorbing carbonaceous using the measured aerosol optical properties and number size distributions, Atmos. Chem. Phys., 12, 2381-2397, 10.5194/acp-12-2381-2012, 2012.

Ma, N., Zhao, C., Tao, J., Wu, Z., Kecorius, S., Wang, Z., Größ, J., Liu, H., Bian, Y., Kuang, Y., Teich, M., Spindler, G., Müller, K., van Pinxteren, D., Herrmann, H., Hu, M., and Wiedensohler, A.: Variation of CCN activity during new particle formation events in the North China Plain, Atmos. Chem. Phys., 16, 8593-8607, 10.5194/acp-16-8593-2016, 2016.

Murphy, D. M., Thomson, D. S., and Mahoney, M. J.: In Situ Measurements of Organics, Meteoritic Material, Mercury, and Other Elements in Aerosols at 5 to 19 Kilometers, Science, 282, 1664-1669, 10.1126/science.282.5394.1664, 1998.

Petters, M. D., and Kreidenweis, S. M.: A single parameter representation of hygroscopic growth and cloud condensation nucleus activity, Atmospheric Chemistry and Physics, 7, 1961-1971, 2007.

Petters, M. D., Carrico, C. M., Kreidenweis, S. M., Prenni, A. J., DeMott, P. J., Collett, J. L., and Moosmüller, H.: Cloud condensation nucleation activity of biomass burning aerosol, Journal of Geophysical Research: Atmospheres, 114, n/a-n/a, 10.1029/2009JD012353, 2009.

Pinnick, R. G., Jennings, S. G., and Chýlek, P.: Relationships between extinction, absorption, backscattering, and mass content of sulfuric acid aerosols, Journal of Geophysical Research: Oceans, 85, 4059-4066, 10.1029/JC085iC07p04059, 1980.

Quinn, P. K., Bates, T. S., Baynard, T., Clarke, A. D., Onasch, T. B., Wang, W., Rood, M. J., Andrews, E., Allan, J., Carrico, C. M., Coffman, D., and Worsnop, D.: Impact of particulate organic matter on the relative humidity dependence of light scattering: A simplified parameterization, Geophys. Res. Lett., 32, n/a-n/a, 10.1029/2005GL024322, 2005.

Rose, D., Nowak, A., Achtert, P., Wiedensohler, A., Hu, M., Shao, M., Zhang, Y., Andreae, M. O., and Pöschl, U.: Cloud condensation nuclei in polluted air and biomass burning smoke near the mega-city Guangzhou, China – Part 1: Size-resolved measurements and implications for the modeling of aerosol particle hygroscopicity and CCN activity, Atmos. Chem. Phys., 10, 3365-3383, 10.5194/acp-10-3365-2010, 2010.

Seinfeld, J. H., and Pandis, S. N.: Atmospheric chemistry and physics: from air pollution to climate change, John Wiley & Sons, 2006.

Su, H., Rose, D., Cheng, Y. F., Gunthe, S. S., Massling, A., Stock, M., Wiedensohler, A., Andreae, M. O., and Pöschl, U.: Hygroscopicity distribution concept for measurement data analysis and modeling of aerosol particle mixing state with regard to hygroscopic growth and CCN activation, Atmos. Chem. Phys., 10, 7489-7503, 10.5194/acp-10-7489-2010, 2010.

Tao, J. C., Zhao, C. S., Ma, N., and Liu, P. F.: The impact of aerosol hygroscopic growth on the single-scattering albedo and its application on the NO2 photolysis rate coefficient, Atmos. Chem. Phys., 14, 12055-12067, 10.5194/acp-14-12055-2014, 2014.

Titos, G., Lyamani, H., Cazorla, A., Sorribas, M., Foyo-Moreno, I., Wiedensohler, A., and Alados-Arboledas, L.: Study of the relative humidity dependence of aerosol light-scattering in southern Spain, Tellus Ser. B-Chem. Phys. Meteorol., 66, 15, 10.3402/tellusb.v66.24536, 2014.

Titos, G., Cazorla, A., Zieger, P., Andrews, E., Lyamani, H., Granados-Muñoz, M. J., Olmo, F. J., and Alados-Arboledas, L.: Effect of hygroscopic growth on the aerosol light-scattering coefficient: A review of measurements, techniques and error sources, Atmospheric Environment, 141, 494-507, http://dx.doi.org/10.1016/j.atmosenv.2016.07.021, 2016.

Wex, H., Neususs, C., Wendisch, M., Stratmann, F., Koziar, C., Keil, A., Wiedensohler, A., and Ebert, M.: Particle scattering, backscattering, and absorption coefficients: An in situ closure and sensitivity study, Journal of Geophysical Research-Atmospheres, 107, 18, 10.1029/2000jd000234, 2002.

Wu, Z. J., Zheng, J., Shang, D. J., Du, Z. F., Wu, Y. S., Zeng, L. M., Wiedensohler, A., and Hu, M.: Particle hygroscopicity and its link to chemical composition in the urban atmosphere of Beijing, China, during summertime, Atmos. Chem. Phys., 16, 1123-1138, 10.5194/acp-16-1123-2016, 2016.

You, Y., Smith, M. L., Song, M., Martin, S. T., and Bertram, A. K.: Liquid–liquid phase separation in atmospherically relevant particles consisting of organic species and inorganic salts, International Reviews in Physical Chemistry, 33, 43-77, 10.1080/0144235X.2014.890786, 2014.

Zhang, L., Sun, J. Y., Shen, X. J., Zhang, Y. M., Che, H., Ma, Q. L., Zhang, Y. W., Zhang, X. Y., and Ogren, J. A.: Observations of relative humidity effects on aerosol light scattering in the Yangtze River Delta of China, Atmos. Chem. Phys., 15, 8439-8454, 10.5194/acp-15-8439-2015, 2015.

Zhao, C., Tie, X., and Lin, Y.: A possible positive feedback of reduction of precipitation and increase in aerosols over eastern central China, Geophys. Res. Lett., 33, L11814, 10.1029/2006GL025959, 2006.

Zieger, P., Fierz-Schmidhauser, R., Weingartner, E., and Baltensperger, U.: Effects of relative humidity on aerosol light scattering: results from different European sites, Atmos. Chem. Phys., 13, 10609-10631, 10.5194/acp-13-10609-2013, 2013.

Zieger, P., Fierz-Schmidhauser, R., Poulain, L., Muller, T., Birmili, W., Spindler, G., Wiedensohler, A., Baltensperger, U., and Weingartner, E.: Influence of water uptake on the aerosol particle light scattering coefficients of the Central European aerosol, Tellus Ser. B-Chem. Phys. Meteorol., 66, 10.3402/tellusb.v66.22716, 2014.

Atmos. Chem. Phys. Discuss., doi:10.5194/acp-2016-1066, 2017
Manuscript under review for journal Atmos. Chem. Phys.
Published: 6 February 2017

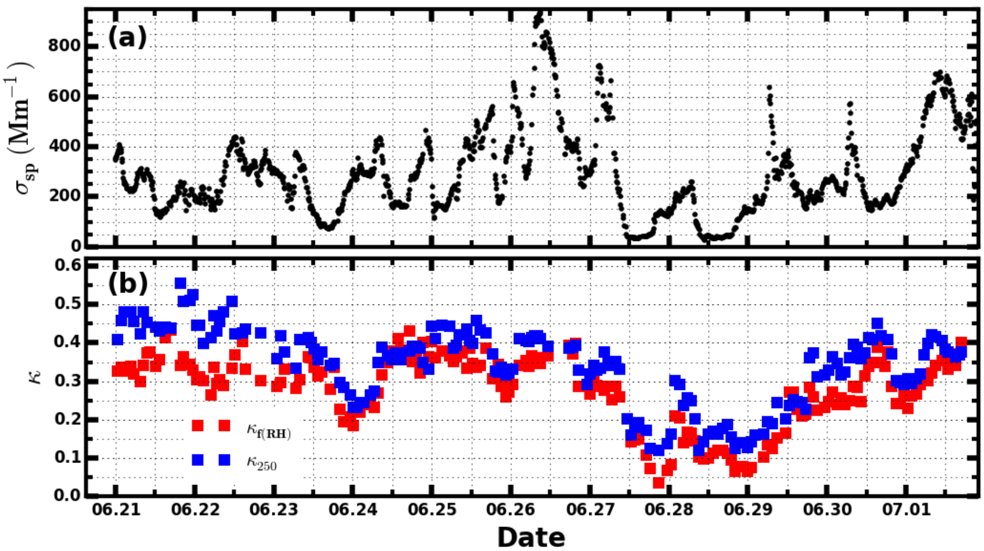

Figure 1. (a) The time series of σ_{sp} at 550 nm; (b) The time series of κ values derived from f(RH) measurements ($\kappa_{f(\text{RH})}$) by combining information of PNSD and BC, and time series of average κ values of aerosol particles at 250 nm (κ_{250}) which is calculated from measurements of HH-TDMA.

Atmos. Chem. Phys. Discuss., doi:10.5194/acp-2016-1066, 2017
Manuscript under review for journal Atmos. Chem. Phys.
Published: 6 February 2017

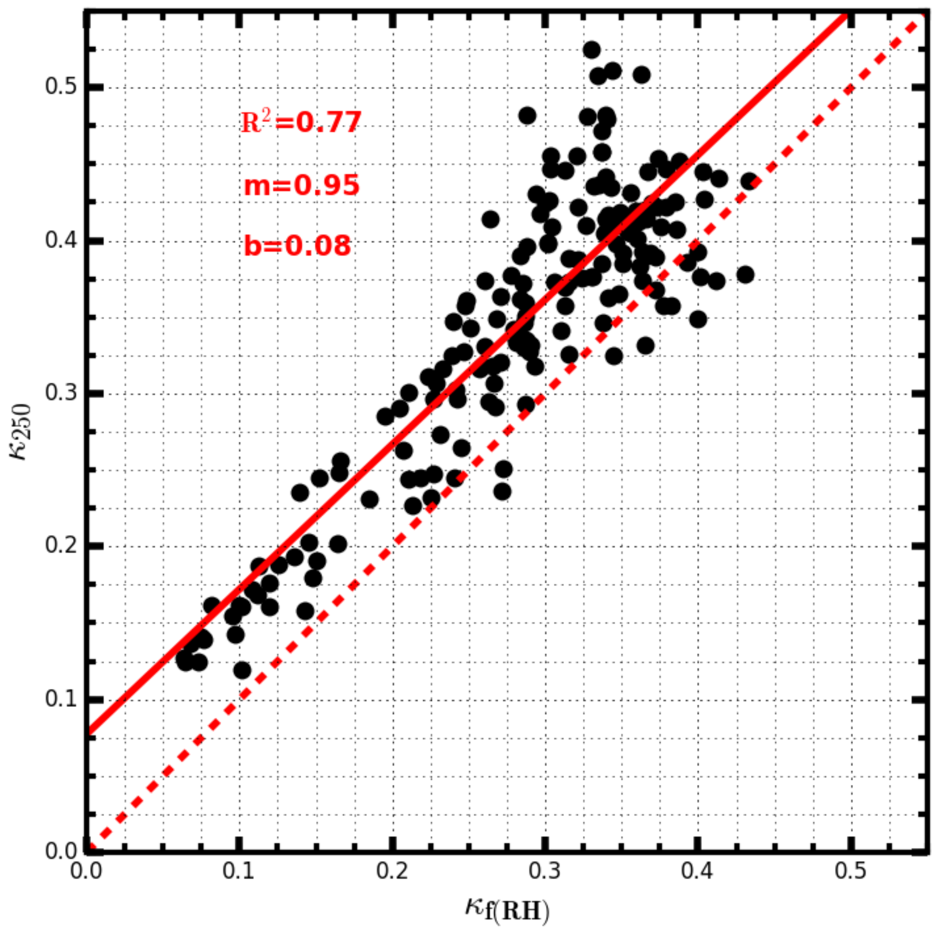

606
607 **Figure 2**. The comparison between κ values derived from $f(\mathrm{RH})$ measurements ($\kappa_{f(\mathrm{RH})}$) and average κ values for aerosol particles with a diameter of 250 nm (κ_{250}) which are derived from measurements of HH-TDMA. R^2 is the square of correlation coefficient, m is the slope and b is the intercept.

Atmos. Chem. Phys. Discuss., doi:10.5194/acp-2016-1066, 2017
Manuscript under review for journal Atmos. Chem. Phys.
Published: 6 February 2017

Atmospheric Chemistry and Physics
Discussions

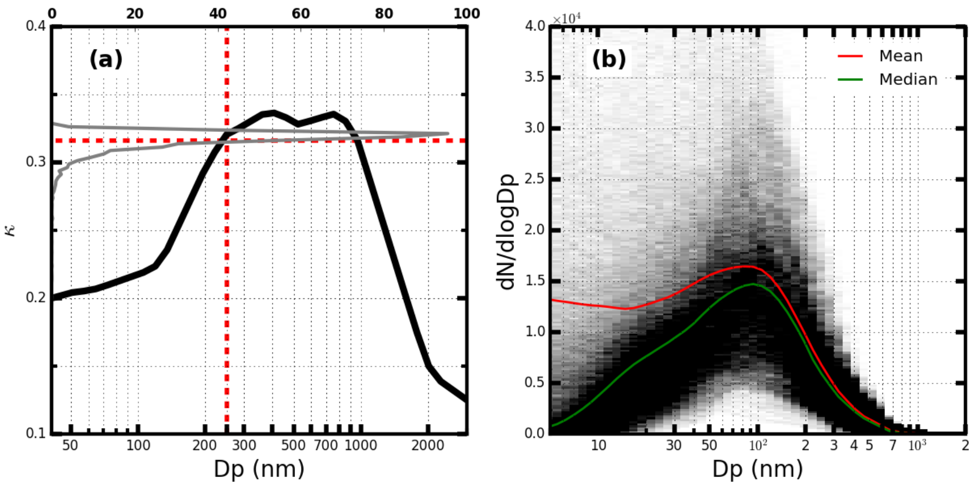

Figure 3. (a) The thick black line represents the average size-resolved κ distribution from HaChi campaign. The solid gray line represents the probability distribution of retrieved κ values with this size-resolve κ distribution by using all PNSDs shown in figure (b), and the horizontal dashed line represents their average. The vertical dashed red line represents the position of 250 nm. (b) All PNSDs which are observed from three different representative background sites of the NCP during summer, they are used to model relationship between size-resolved $\kappa$and retrieved κ values from $f(\mathrm{RH})$ measurements, and the gray color represents the frequency of PNSD, darker point corresponds to higher frequency, red and green line represent mean of median values of all observed PNSDs.

Atmos. Chem. Phys. Discuss., doi:10.5194/acp-2016-1066, 2017
Manuscript under review for journal Atmos. Chem. Phys.
Published: 6 February 2017

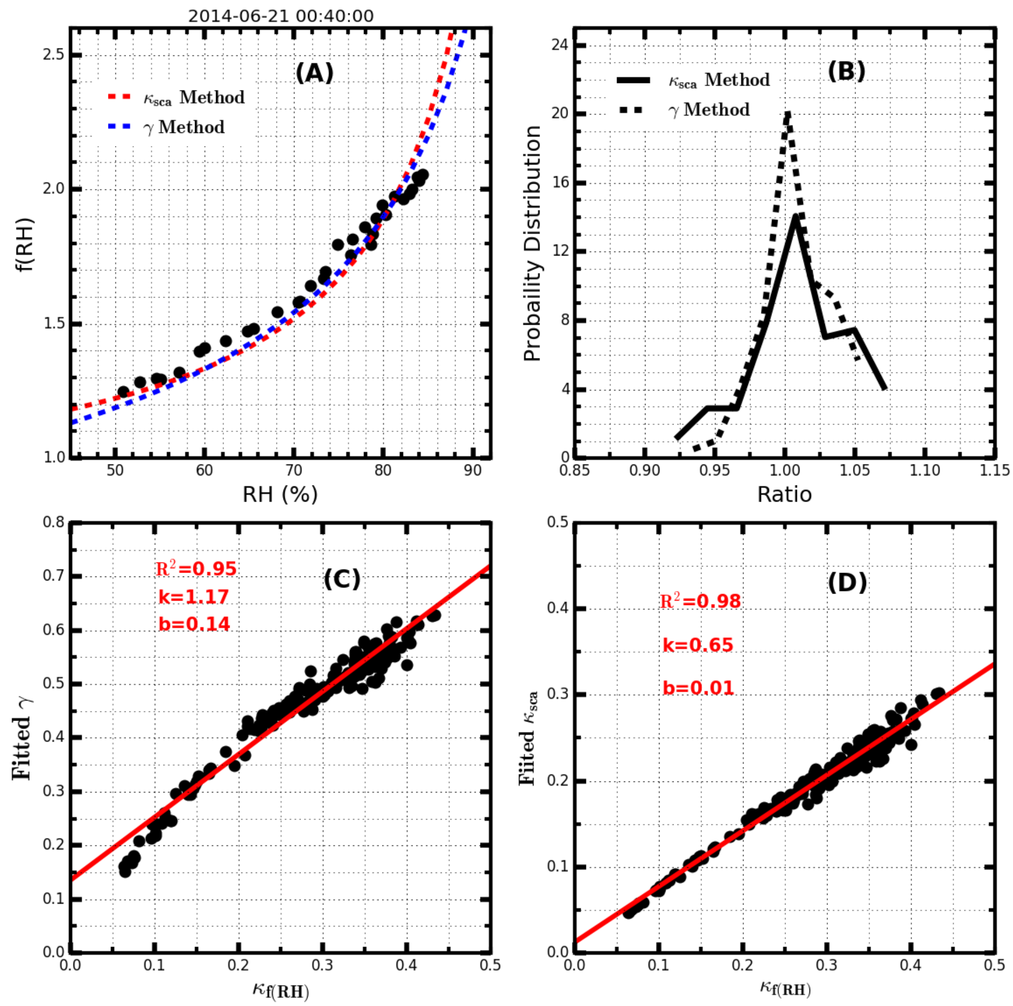

Figure 4. (A) Fitting example of two discussed parameterization schemes, and title shows the observation time of this $f(\mathrm{RH})$ curve; (B) The fitting performance of two discussed parameterization schemes, x-axis represents the ratio between fitted $f(85\%)$ and measured $f(85\%)$ and y-axis represents the probability distribution. (C) The linear relationship between values of $\kappa_{f(\mathrm{RH})}$ and fitted γ, R^2 is the square of correlation coefficient, k is the slope and b is the intercept; (D) The linear relationship between values of $\kappa_{f(\mathrm{RH})}$ and fitted κ_{sca}.

Atmos. Chem. Phys. Discuss., doi:10.5194/acp-2016-1066, 2017
Manuscript under review for journal Atmos. Chem. Phys.
Published: 6 February 2017

Atmospheric Chemistry and Physics
Discussions
Open Access

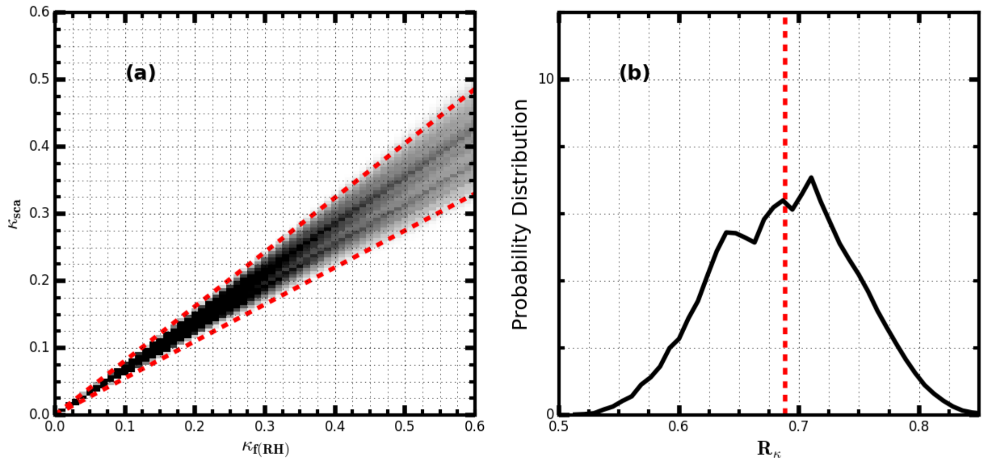

Figure 5. (a) Simulated relationships between $\kappa_{f(\mathrm{RH})}$ and κ_{sca} under different PNSD conditions (all PNSDs shown in Fig.3a are used as inputs to conduct the simulation experiment), gray color represents the frequency and darker point corresponds to higher frequency, the slope of two dashed lines are 0.55 and 0.81; (b) The probability distribution of R_κ ($\kappa_{sca}/\kappa_{f(\mathrm{RH})}$).

Atmos. Chem. Phys. Discuss., doi:10.5194/acp-2016-1066, 2017
Manuscript under review for journal Atmos. Chem. Phys.
Published: 6 February 2017

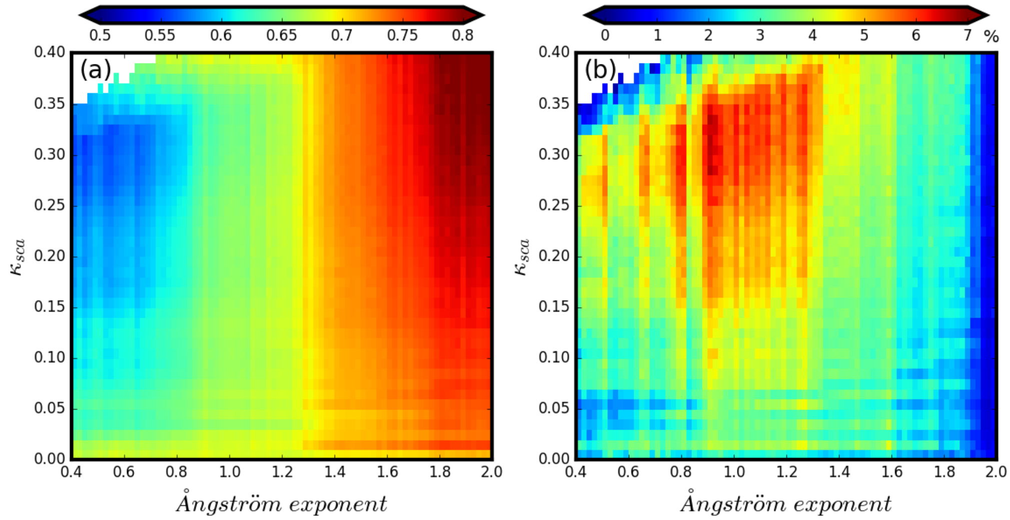

Figure 6. (a) Colors represent R_κ values and the color bar is shown on the top of this figure, x-axis represents Ångström exponent and y-axis represents κ_{sca}. (b) Meanings of x-axis and y-axis are same with them in (a), however, color represents the percentile value of the standard deviation of R_κ values within each grid divided by their average.

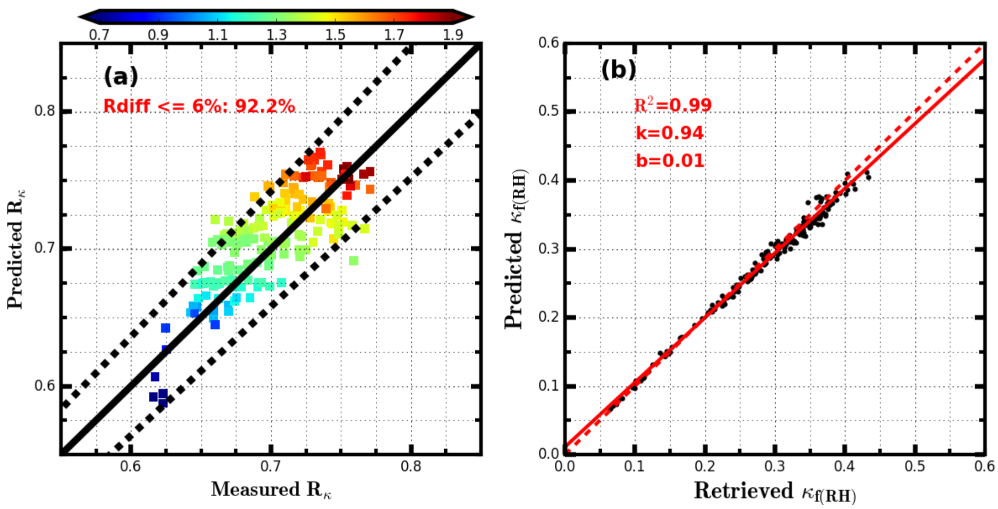

Figure 7. (a) The comparison between measured and predicted R_κ values, colors represent values of Ångström exponent, texts with red color show the percentile of points with relative difference (Rdiff) less than 6% , two dashed line are lines with absolute relative difference (Rdiff) equal to 6% ; (b) the comparison between retrieved $\kappa_{f(\mathrm{RH})}$ values by using traditional method introduced in Sect.3.1 and predicted $\kappa_{f(\mathrm{RH})}$ by using the new method introduced in Sect.4.3, R^2 is the square of correlation coefficient, k is the slope and b is the intercept.